Ink-Jet Printer's Characterization by 3D Gradation Trajectories on an Equidistant Color Difference Basis

Oleg Milder[1] and Dmitry Tarasov[1,2(✉)]

[1] Institute of Radio-Engineering and IT, Ural Federal University, Mira, 32, Ekaterinburg 620002, Russia
datarasov@yandex.ru
[2] Institute of Industrial Ecology UB RAS, Kovalevskoy, 20, Ekaterinburg 620990, Russia

Abstract. We suggest using 3D gradation curves of CIE *Lab* space, which we call "gradation trajectories", as further development of common gradation curves. The trajectories are considered in terms of 3D curves of differential geometry. We offer the gradation trajectories, as well as their calculating method, as a powerful tool for ink-jet system characterization and further profile-making. In the work, we develop our method and apply it to ink-jet printer's characterization on a basis of equidistant color difference CIE *Lab* ΔE. We discuss the information that might be derived from the trajectories' analysis and show how they might me generally applicable.

Keywords: Gradation trajectories · Ink-jet · Characterization · Profile Dot–gain

1 Introduction

In order to create images with faithfully reproduced colors on a given ink-jet printer system, it is essential to specify the color response the printer provides for a given selection of substrate (e.g. paper), inks types, and with given amounts of inks during the process of characterization.

The limitation of ink serves to doze the amount of ink that can be sent to the print head by the raster processor (RIP), and to reduce the desired or useful percentage of ink, which can often be less than 100%. Need of such a restriction caused by many factors, particularly the physics-chemical processes of interaction between inks and substrates, primarily for non- or weak-absorbing ones. When several dyes are being printed on top of each other, there is a limit on the amount of ink that can be applied to the substrate and on the previous color layer. When this technical restriction is ignored, the ink that stacks last will not properly attach to the previous layers, which will lead to dirty brown shades in the neutral tints. The ink will also not dry properly. This can cause set-off where the ink of a still wet substrate rubs off on whatever is stacked on top of it. In general, due to the printing process, the deposited ink surface coverage is larger than the nominal

M. Paul et al. (Eds.): PSIVT 2017, LNCS 10749, pp. 40–52, 2018.
https://doi.org/10.1007/978-3-319-75786-5_4

coverage, resulting in a physical dot-gain responsible for the ink spreading, which depends on the inks, on the substrate, and also on some other factors [1].

There is a systemic contradiction in the market. While manufacturers want to boost the ink usage, customers would like to reduce ink consumption with minimal impact on color quality. Sometimes, these limitations lead to loss in color. In any case, the problem of ink management is crucial. To solve this problem, manufacturers of image processing software and printing equipment recommend using different criteria, such as: visual evaluation by spreading or capillarity, numerical estimation of the optical density of color coordinates, etc.

Thanks to different color prediction models (CPMs) or reflectance prediction models (RPMs), the usage of inks can be substantially optimized especially in the case of current multi-colors printers. CPMs may help the image processing software to decide, which set of inks and how to select in order to print a certain color within a specific context. Such models need to account for both the interactions between the inks and the substrate and between the light and the halftone print, as well as the Fresnel reflections and light scattering. The lateral light scattering together with internal reflections at the interface between the substrate and the air are responsible for the optical dot gain effect.

1.1 Color Prediction Models

Today, a great deal of CPMs exists. The models take as their inputs a set of ink values and predict the resulting color in print, as specified by reflectance models or tristimulus values. *Empirical surface models* take into account superpositions of ink halftones. There, reflected or transmitted light is supposed to be a function of the effective colorants surface coverage or base patterns forming ink halftones. The models do not deal with the light propagation and fading within the print and only demonstrate the relationship between reflected light and surface coverages by colorants. *Physically inspired models* engage a more detailed analysis of light-print interaction based on mathematical prediction of how light paths within a halftone print go and what resulting fade is. *Ink spreading models* are designed to characterize the effective surface of a colorant/ink dot after it has been printed at a given nominal surface coverage. The difference between the effective and the nominal surface coverages is the physical dot gain, which show how much a colorant/ink dot spreads out. Ink spreading models accounting for ink spreading in all ink superposition conditions. They rely on ink spreading curves mapping nominal surface coverages to effective surface coverages for the surface coverages of single ink halftones, as well as ones superposed with single and two solid inks.

More complicated up-to-date CPMs deal with spread-based and light propagation probability, as well as light transportation. Moreover, the best accuracy in models reaches by implicating the hybridization. *Spectral reflection prediction models* (SRPM) are helpful in studying the impact of different factors influencing the range of printable colors (the inks, the substrate, the illumination conditions, and the halftones) and in creating printer characterization profiles for the purpose of color management [2]. The Kubelka–Munk model (1) is widely used to predict the properties of multiple layers of ink overlaid at a given location, given information about each constituent ink's reflectance and opacity [3].

$$\frac{K(\lambda)}{S(\lambda)} = \frac{(1 - R_{\infty}(\lambda))^2}{2R_{\infty}(\lambda)} \tag{1}$$

where K is absorption and S is scattering coefficients, R_{∞} is the reflectance of an infinitely thick sample and the prediction of S and K from reflectance is made at a given wavelength λ. The formula (1) allows predicting the combined K and S coefficients for multiple inks:

$$K(\lambda) = K_B(\lambda) + \sum\nolimits_{i=1}^{l} c_i K_i(\lambda) \tag{2}$$

where B refers to the substrate, l is the number of ink layers, c_i is the concentration and K_i is the absorption coefficient of the i-th layer. $S(\lambda)$ is computed analogously.

One of the first integrated CPM is the Neugebauer model, which predicts the CIE *XYZ* tristimulus values of a color halftone patch as the sum of the tristimulus values of their individual colorants [4]. Since the Neugebauer model does not take into account the lateral propagation of light within the paper and internal reflections at the paper-air interface, its predictions are considered inaccurate.

The most well-known SRPM among recent ones is the Yule–Nielsen modified spectral Neugebauer model (YNSN) where the Yule–Nielsen relationship applied to the spectral Neugebauer equations [5, 6].

$$R(\lambda) = \left(\sum\nolimits_{i=1}^{p} w_i P_i(\lambda)^{\frac{1}{n}}\right)^n \tag{3}$$

where $R(\lambda)$ is the reflectance of a halftone pattern neighborhood that is optically integrated as it is being viewed, w_i is the relative area coverage of the i-th *Neugebauer primary* – P, n is the Yule-Nielsen non-linearity that accounts for optical dot gain.

The further enhancement of the model (EYNSN) accounts the ink spreading effect connected with the respective physical dot-gains of one ink halftone printed in different superposition conditions (single colorant and its combinations with 1–3 another colorants). The model uses multiple ink spreading curves (tone reproduction curves, TRC) to characterize the physical dot-gain of the ink halftones on substrate and in all solid ink superposition conditions [7]. Spectral reflection prediction models together with ink-spreading models accounting for physical dot-gain are able to predict reflectance spectra as a function of ink surface coverage for 3–4 inks [1, 8]. Minimization of difference metric between measured and predicted reflection spectrum for each superposition condition takes the effective ink surface coverage and the ink-spreading curve mapping nominal to effective surface coverage for each colorant.

1.2 Literature Review

Different CPMs have been successfully applied to color predictions in various contexts. Some studies inspired us to do the research into the development of this topic.

The work [9] devoted to calibrating the YNSN model with ink spreading curves derived from digitized RGB calibration patch images. Researchers carry out spectral predictions with the ink spreading curves calibrated by relying on RGB images of 36 C, M, and Y patches (without black channel). For calculating the ink spreading curves, 25%, 50%, and 75% nominal coverage are used in each superposition condition. In addition, for the broadband Yule–Nielsen equation [7, 10], they used the digitized RGB images of the paper white, the solid inks, and all the solid ink superposition. The model is tested on 729 patches comprising all nominal surface coverage combinations of 0%, 13%, 25%, 38%, 50%, 63%, 75%, 88%, and 100%. For the comparison, authors offer the prediction accuracies with the calibration of the ink spreading curves performed by spectral fits according to the YNSN model. As a reference, they consider also a single ink spreading function per ink obtained by computing the effective surface coverage of single ink halftones printed on paper. The prediction results demonstrate that the full ink-spreading model deduced from RGB images yields a better prediction accuracy than the classical single ink dot-gain relying on spectral fits. The full ink-spreading model relying on digitized RGB images shows a slightly lower accuracy compared with the one calibrated with measured reflection spectra.

Thus, authors reduce the effort of calibrating the YNSN model accounting for full ink spreading by computing the nominal to effective surface coverage curves from digitized RGB images instead of measured reflection spectra. For the calibration of the model by digitized RGB images, a user needs to measure only the reflection spectra of the solid colorant patches (for 3 inks: 8 patches) and digitize one sheet containing all calibration patches (for 3 inks: 44 patches). By using images instead of spectra, the prediction accuracy is not much affected. Tests are carried out with 729 color patches covering the complete gamut of the output device. In case of C, M, and Y ink, the mean CIE *Lab* ΔE_{94} difference between predicted and measured reflection spectra for calibration by spectral fits was 1.00. When calibrating with digitized RGB images, the mean prediction difference is CIE *Lab* $\Delta E_{94} = 1.29$.

Livens [11] describes multi-density ink calibration in a framework that includes ink limitation and characterization and proposes a technique called multiple characterization, which allows to achieve a predefined color response with respect to more than one quantity, by exploiting the additional degrees of freedom offered by similarly colored inks. The method aims to improve the visual uniformity. It is noted that the process of ink transition management must be under strict control since the transition between light and dark inks could result in some artefacts caused by too large amount of ink. However, a key characteristic of existing ink mixing solutions is that they define the mapping in a fixed way, independent of the calibration. The mapping is usually empirically optimized for a certain condition of the printer that might vary over time.

The author proposes to replace the fixed ink mixing by a calibrated ink mixing implies the multiple characterization, in which ink increments are computed that correspond to equal increments or decrements in the measured variable, however, the measured value implies a set of different solutions, corresponding with various ratios of light and dark inks. The choice is done by constructing a calibration that results in more uniform CIE *Lab* ΔE steps. The characterization covers only that pair of CIE *Lab* coordinates (L, a, b) which contributes much more to CIE *Lab* ΔE. In fact, the major contribution is made by the chromatic coordinate (a, b). In geometrical interpretation, with single and multi-density inks, a 1D trajectory is described in the 3D color space by varying the ink percentage.

The author suggests the characterization means dividing the trajectory into steps that correspond to an equal change in a measured variable. He also agrees that it is often useful or even necessary to set ink limitations in order to cut off areas that cause problems in characterization. However, there is no description of curves behavior and no suggestions how to manage ink limits.

In the work [12], the objective is to quantify the influence of ink-jet printer calibration and profile–making on the quality of color reproduction, in the context of fine art printing on a special paper compared with those obtained on a coated paper. The first step of the experiment is a fine setting of the printer, in order to stabilize the results. The second step is a complete printer characterization with profile-making, when different input parameters (total ink coverage, black ink limit, etc.) are adjusted. The performance of the color profiles is analyzed by color differences (CIE *Lab* ΔE), the volume of color gamut, and spectral characteristics of the printed colors. Then the profiles are edited and optimized in order to reduce the color differences.

The authors emphasize the importance of characterization because the tone increase value for ink-jet printing is generally larger than for the other printing processes. They also agree that the determination of the limit total area coverage (TAC) accepted by a paper is crucial in order to avoid problems such as poor ink drying and smudges, and indicate typical value of TAC for ink-jet on coated paper as 250%. Test-charts like IT8 7/3 are pointed to be a possible way for such a determination, as well as for obtaining the grey balance. ICC profiles are expected to be the overriding part of characterization.

During the TAC determination, the amount of ink supply is assessed visually, when for a limit of 280% there is a problem of ink migration towards the adjacent patches. Besides, there is a strong difference with the coated paper which accepts higher ink superimpositions. The best TAC (160%) is chosen by minimal CIE *Lab* ΔE variation. As a result, the work does not demonstrate a substantial scientific novelty, however, showed the typical way by which experts go when calibrate printing equipment.

The paper [13] is connected to ink consumption while achieve an accurate digital color reproduction by an ink-jet printer on different non-paper-substrates of POP display media. The assessments are done by measuring by a spectrophotometer raw characterization targets, which display color cast. The ink usage is determined in terms of amount of ink restriction. A characterization test target is used to exam the ink-jet hooking phenomena, i.e. the ink hue shifting associated with ink-jet printers. It is noted that the color shift happens in chromatic and neutral shadow areas of a print due to impurities in the ink-jet inks. For a particular substrate, a typical ink-jet hooking phenomenon (for C and M channels) is observed when printing with full ink load (see Fig. 1(a)).

It shows the hue angle of Cyan color begins to shift from a cyan blue to a contaminated cyan that turns purple because there is more red color in the cyan. The hue angle of magenta color shifts toward yellow. With further ink restriction (−16.25%), the ink-jet hooking is reduced, and ink distributed more evenly and correctly on the media (see Fig. 1(b)). At the same time, ink restriction reduces the size of the color gamut: 16.25% ink reduction cut down the size of color gamut about 9%. A similar effect is observed for another substrates. It is concluded that it is necessary to experiment with different characterization settings to achieve the right amount of ink distributed on the media. Each individual ink channel should be restricted just right after the color begins to change "hook" from the base primary color, while leaving extra color to extend the gamut for spot colors. Despite observation the phenomena, the author does not reveal the cause and offers only empirical estimates of ink reduction.

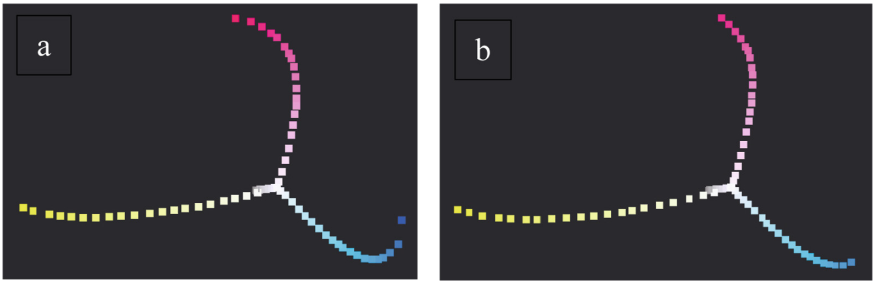

Fig. 1. Color hooking phenomena before (a) and after (b) ink reduction (Color figure online)

The described approach might be promising; however, it cannot be applied without correcting its shortcomings. The major one is the fact that in any case, some information about the color is lost when analyzing the projections on the *ab*-plane, without space considerations. For instance, yellow colorant do not tend to form "hook" on the *ab*-plane, but do it on the *Lb*-plane instead. Unfortunately, it is not reflected in figures, such as Fig. 1.

All mentioned approaches have their advantages as well as drawbacks, too. Majority of models are too complicated to be embedded in a real workflow without substantial development and adjustment that takes time. For instance, YNSN-based models are extremely critical to the selection of the parameter n. Generally accepted algorithms for its definition in the literature are not described. Usually it is suggested to carry out selection by brute force, which is utterly laborious. The empirical approach is more promising, however it requires a large number of printed tests for each pair of substrate-ink. Moreover, so far any complete model that predicts the behavior of ink in terms of its limited supply in inkjet printing has not been proposed.

Gradation scales and gradation-based techniques are known as an indispensable attribute of color printing systems settings [14, pp. 88–89]. At the same time, the authors expresses doubts about the rational use of these characteristics in digital printing technology. The main problem is the fact that using the gradation curves in conventional 2D embodiment significantly reduces the quantity and quality of information extracted from them. In the work [15], 3D gradation trajectories are introduced as a further development of the gradation curves approach. Implication the mathematical apparatus of differential geometry for gradation trajectories analysis in 3D CIE *L, a, b* space allows reveal their intrinsic features of curvature and torsion. The approach used is not a model in the full sense, since it does not use any a priori assumptions. It is only a description of the measurements results in the form of empirical functions.

These features are applied to define the ink limits in ink-jet printing systems and to create the empirical approach based on trajectories' curvature and torsion behavior analysis.

This work is devoted to further development of the proposed technique. We suggest using an equidistant CIE *Lab* ΔE color difference as a basement for ink-jet printers' characterization with help of 3D gradation trajectories. We offer a simple approach for such a characterization, which implies a small number of prints and rapid calculations.

2 Approach

The approach we describe as follows. Print specially developed test chart → Measure *Lab* coordinates of the chart with a spectrophotometer → Sorting data by color channels in order of increasing percentage of fill → Curve fitting by a polynomial of fourth degree → Curvature analysis, definition of the ink limitation point → Calculation of the arc length of a curve from 0 to the point corresponding to curvature's maximum → The curve is divided to segments based on the equal color difference → Print test chart to assess the result.

First, we introduce gradation trajectories. Let's a gradation trajectory is the locus of points in the CIE *Lab* space, which coordinates are consistent with the individual fields of measurement of the tone scale, arranged in ascending order of percentage of raster cells coverage in the layout of 0% (unsealed substrate) to 100% (dye). Tone scales generally comprise no more than two dozen of fields, i.e. in practice; the gradation trajectory is represented by a discrete set of points in CIE *Lab* space. Modern printing systems provide a color depth of at least 256 gradations (8 bits), i.e. color change characteristics (hue, saturation and brightness), as well as the color coordinates, might be assumed as a continuous function of the percentage (proportion) of raster cell filling. In other words, we can expect a nearly continuous change of color characteristics when filling percentage of a raster cell changes continuously.

If we took the percentage of raster cell filling as a parameter of a curve t, the gradation trajectory might be set by the parametric equations (4):

$$\begin{cases} t \in [0;\ 1] \\ L = c_{4L} \cdot t^4 + c_{3L} \cdot t^3 + c_{2L} \cdot t^2 + c_{1L} \cdot t + c_{0L} \\ a = c_{4a} \cdot t^4 + c_{3a} \cdot t^3 + c_{2a} \cdot t^2 + c_{1a} \cdot t + c_{0a} \\ b = c_{4b} \cdot t^4 + c_{3b} \cdot t^3 + c_{2b} \cdot t^2 + c_{1b} \cdot t + c_{0b} \end{cases}, \tag{4}$$

where $c_{ij}(i = \overline{1,2,3,4}; j = \overline{L,a,b}$ are some numerical coefficients, c_{0j} are *Lab*-coordinates of unsealed substrate. The interval of parameter t alteration is accepted from 0 (unsealed substrate) to 1 (100% dye).

Since we have agreed to assume the functions (1) to be continuous on the segment, then, according to the Weierstrass approximation theorem [16], their analytical form could be given by a polynomial of a certain extent. The theorem proves that if f is a continuous real-valued function on $[a, b]$, and if any $\varepsilon > 0$ is given, then there a polynomial p on $[a, b]$ such that $|f(x) - p(x)| < \varepsilon$ for all x in $[a, b]$ exists. In words, any continuous function on a closed and bounded interval can be uniformly approximated on that interval by polynomials to any degree of accuracy. In our case, the polynomial of the fourth power is required to detect such features of a space curve as the curvature (κ) [17, p. 49], because in the process of calculating, the derivatives respect to a parameter up to the second power are used:

$$\begin{gathered} r = (a(t),\ b(t),\ L(t)) \\ \kappa = \frac{|r' \times r''|}{|r'|^3} \end{gathered} \tag{5}$$

Ink spreading on solid surfaces and penetration into porous matrices (coated and uncoated papers) describes by power-law exponents [18]. However, for coated papers polynomials of the fourth power give satisfactory approximation accuracy. In this case, approximation errors are less than measurement ones.

In order to define n equidistant points with respect to ink limitation we first need to evaluate trajectory's arc length of a curve S (6). Thus, we discover full tone increase corresponding to t increment, as well as t_x values corresponding to even tone segments (7).

$$S = \int_0^{t_{max}} dE_{94} \tag{6}$$

$$\int_0^{t_x} dE_{94} = \frac{S}{n} \tag{7}$$

3 Experimental Verification

For the experiment, we use the 4-color (CMYK) wide-format solvent ink-jet printer Mimaki CJV30-160BS. Print mode: 720 × 720 dpi, variable dot. Substrate: coated paper MediaPrint Gloss 150 g/m^2 as a weak-absorbent substrate. The measurement tools: spectrophotometer x-Rite iOne iSis + x-Rite ProfileMaker package.

Tone scales containing 20 bitmap fields are synthesized using a ChartGenerator/MeasureTool in ProfileMaker design for the automatic iOne iSis (see Fig. 2, above). Sample scales are printed by "swastika" on the same sheet in order to average the results of scale measurement depending on the print direction and printing head movement in relation to the layout.

The results of the 4 measurements are averaged in ProfileMaker/MeasureTool and save as a text file, which then imports into MS Excel, where it stay out as a matrix of variables of dimension 21 (20 raster fields plus the unsealed substrate) × 4 (the proportion of a raster cell filling plus CIE *Lab* coordinates values). Measured data are divided into individual color channels. Matrix variables, which contained t, L, a, b data of each color patch as columns, are imported in MatLab, where they are carried out in further mathematical processing.

The approximation of dependences (4) by polynomials is implemented in MatLab package using the fit function. It is necessary to ensure a minimum cumulative CIE *Lab* ΔE_{76} [19] color difference between the theoretical trajectory and experimental points. The value of the total color difference CIE *Lab* ΔE_{76} of experimental points from the theoretical trajectory is 2–3 units. For comparison, the worst deviation from the average in the preparation of the experimental points was 3–6 color difference CIE *Lab* ΔE_{76} units. The obtained t_x values (7) are in fact the tone reproduction curves (TRC) points that are further implicated into raster image processor (RIP).

Final evaluation is done by preparation of a new arbitrary scale with 10% tone increase on a color channel (Fig. 2, below) that is further printed out and is measured.

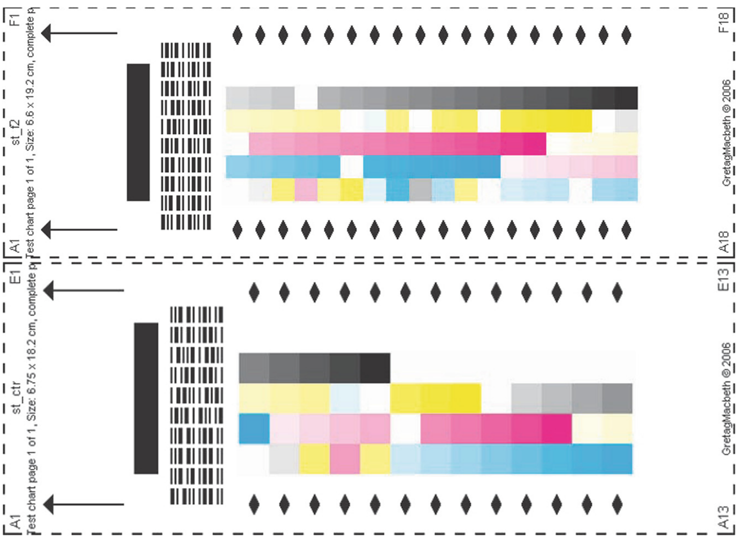

Fig. 2. iOne iSis test charts to print: (above) tone chart for measurement (below) tone chart for evaluation

4 Results and Discussion

As for any other continuous space curve, the numerical factors such as curvature in terms of differential geometry can be defined at each point of the gradation trajectory. Figure 3 shows gradation trajectories for the Cyan and Yellow color channels (as for instance). The dots correspond to the tone scale fields variation, solid curve is an approximating gradation trajectory, a projection of the actual measurements on the *ab* chromaticity plane is shown at the bottom. Obviously, the points corresponding to an equal tone increase (+0.05) are located on the trajectory not equidistantly.

Figure 4 shows the dependencies of curvature on the part of tone. As can be seen, the curvature of the trajectory is different from zero in a narrow band of the range. The presence of local extrema points to a jerky change of hue while a raster cell is being filled. For the further calculations, the ink limits are set to 83.67% for the Cyan channel and to 85.17% for the Yellow channel .

Figure 4 shows a part of the curvature graph that is significantly different from zero. The maximum of curvature corresponds to the region of the sharpest bending of the gradation path, i.e. the sharpest change in color tone for the Cyan channel and the sharpest drop in brightness for the Yellow channel. These are the points that are chosen to limit the maximum ink supply for the specified color channels. In addition, this tone value is utilized as the upper limit of integration (t_{max}) in (6) for the further calculation.

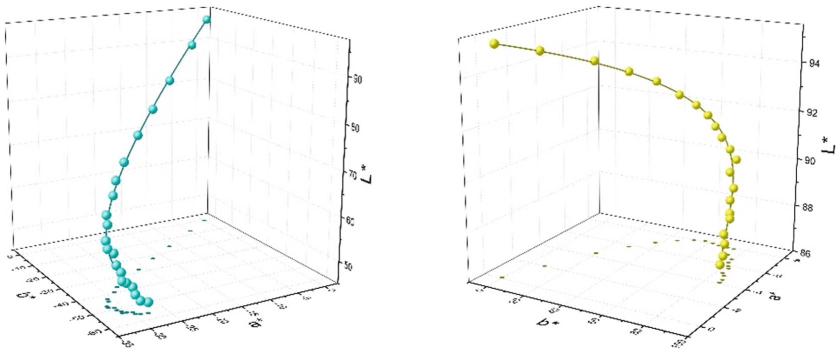

a) b)

Fig. 3. Gradation trajectory for the (a) cyan and (b) yellow channels (Color figure online)

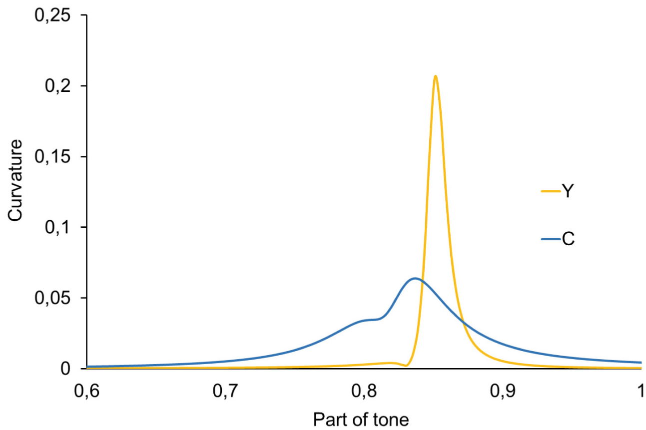

Fig. 4. Curvature values for the gradation trajectory depending on the part of tone (Color figure online)

Figure 5 shows *Lab*-coordinates of measured test patches, which correspond to 0.1 tone increment on the gradation trajectory after characterization for the Cyan and Yellow channels. The dots lie exactly on the calculated trajectory for both channels.

Arc lengths of curves of segments connecting neighbor dots are more equal than ones indicated in Fig. 3. This also is demonstrated in Fig. 6 where color differences that correspond to the related arc length seem to be the same.

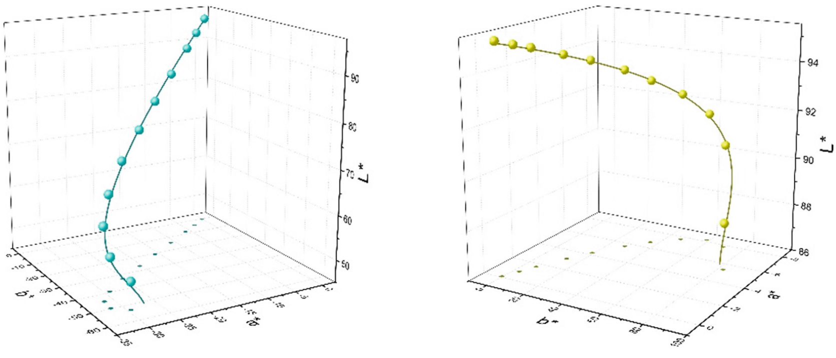

a) b)

Fig. 5. Measured points on gradation trajectory after characterization for the (a) cyan and (b) yellow channels (Color figure online)

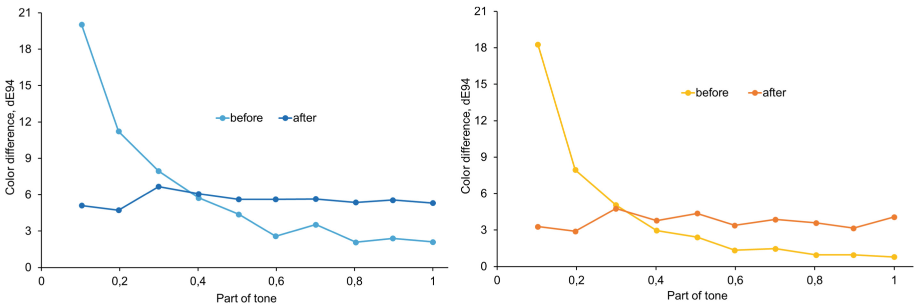

a) b)

Fig. 6. CIE *Lab* ΔE_{94} color difference between patches, which correspond to 0.1 tone increment before and after characterization for the (a) cyan and (b) yellow channels (Color figure online)

5 Conclusion

A new three-dimensional interpretation of the gradation curves in CIE *Lab*-space is proposed. Gradation trajectories, as well as the method of their analytical description, are described. Gradational trajectories are conceived as continuous, bounded on the gradation range curves. In this connection, the apparatus of differential geometry of curves is applied to them, and the values of such parameters as curvature and arc length of a curve are calculated.

Gradation trajectories introduced by the described manner are the global features of ink-jet printing process that are depended on type of a substrate and properties of the ink only. They are not affected by rasterizing method, number of passes and measuring technique.

Recently, there was no sustainability criterion, which can be applied for certain specification of maximum percentage of the ink supply. Possible options for such a criterion might be a first maximum in the plot of gradation trajectory's curvature.

The arc length of a curve of the trajectory might be utilized as a powerful and fast-acting tool for ink-jet systems characterization.

Any limitation of ink supply and any method of characterization under the conditions of a tone scales print will give the family of the points belonging to the gradation trajectory. In other words, if the printing conditions mentioned are met, then regard-less of the selected ink supply limitations, the results of measurement of gradation scales will form a family of points on the gradation trajectories describing each color channel.

Since the described approach is not a model, the results cannot be compared to any CPM. The approach ensures reproduction of a given tint with accuracy to the quantization error. In the case of 8-bit color, the nearest of 256 possible halftones is selected. The further development of the approach implies introduction of 3D gradation surfaces as a method describing interconnection between two colorants, especially in the case of regular and light inks pairs.

References

1. Balasubramanian, R.: Optimization of the spectral Neugebauer model for printer characterization. J. Electron. Imaging **8**, 156–166 (1999)
2. Bala, R.: Device characterization. In: Sharma, G. (ed.) Digital Color Imaging Handbook, pp. 269–379. CRC Press, Boca Raton (2003)
3. Kubelka, P., Munk, F.: Ein Beitrag zur Optik der Farbanstriche. Zeitschrift für technische Physik **12**, 593–601 (1931). Germany
4. Neugebauer, H.E.J.: Die theoretischen Grundlagen des Mehrfarbendrucks. Zeinschrift fur Wissenschaftliche Photographie Photophysik Photochemie **36**, 36–73 (1937)
5. Yule, J.A.C., Nielsen, W.J.: The penetration of light into paper and its effect on halftone reproductions. In: Proceedings of TAGA Conference 1951, pp. 65–76. TAGA, Sewickley (1951)
6. Viggiano, J.A.S.: Modeling the color of multi-colored halftones. In: Proceedings of TAGA Conference 1990, pp. 44–62. TAGA, Sewickley (1990)
7. Hersch, R.D., Crété, F.: Improving the Yule–Nielsen modified spectral Neugebauer model by dot surface coverages depending on the ink superposition conditions. In: Proceedings of SPIE, vol. 5667, pp. 434–445 (2005)
8. Wyble, D.R., Berns, R.S.: A critical review of spectral models applied to binary color printing. Color Res. Appl. **25**, 4–19 (2000)
9. Garg, N.P., Singla, A.K., Hersch, R.D.: Calibrating the Yule–Nielsen modified spectral Neugebauer model with ink spreading curves derived from digitized RGB calibration patch images. J. Imaging Sci. Technol. **52**(4), 040908-1–040908-5 (2008)

10. Arney, J.S., Engeldrum, P.G., Zeng, H.: An expanded Murray-Davis model of tone reproduction in halftone imaging. J. Imaging Sci. Technol. **39**, 502–508 (1995)
11. Livens, S.: Optimisation of printer calibration in the case of multi density inks. In: Conference on Color in Graphics, Imaging, and Vision, CGIV 2002 Final Program and Proceedings, pp. 633–638 (2002)
12. Chagas, L., Blayo, A., Giraud, P.: Color Profile: methodology and influence on the performance of ink-jet color reproduction. In: IS&T's NIP20: 2004 International Conference on Digital Printing Technologies, pp. 655–659 (2004)
13. Wu, Y.-J.: Reducing ink-jet ink consumption with RIP software for POP display media. In: Digital Fabrication and Digital Printing: NIP30 Technical Program and Proceedings, pp. 108–111 (2014)
14. Kipphan, H.: Handbook of Print Media, p. 1207. Springer, Heidelberg (2001). https://doi.org/10.1007/978-3-540-29900-4
15. Milder, O.B., Tarasov, D.A., Titova, M.Y.: Inkjet printers linearization using 3D gradation curves. In: CEUR Workshop Proceedings. Proceedings of the 1st International Workshop on Radio Electronics & Information Technologies (REIT 2017), Yekaterinburg, Russia, 15 March 2017, vol. 1814, pp. 74–83 (2017)
16. Jeffreys, H., Jeffreys, B.S.: Weierstrass's Theorem on Approximation by Polynomials and Extension of Weierstrass's Approximation Theory, §14.08–14.081 in Methods of Mathematical Physics, 3rd edn, pp. 446–448. Cambridge University Press, Cambridge (1988)
17. Pogorelov, A.V.: Differential geometry. Noordhoff, 171p. (1959). (Translated from Russian)
18. Rosenholm, J.B.: Liquid spreading on solid surfaces and penetration into porous matrices: coated and uncoated papers. Adv. Colloid Interface Sci. **220**, 8–53 (2015)
19. Pauli, H.: Proposed extension of the CIE recommendation on "uniform color spaces, color difference equations, and metric color terms". J. Opt. Soc. Am. **66**, 866–867 (1976)